Examining the Potential of Z_{DR} Columns to Predict Tornado Formation and Intensity in Quasi-Linear Convective Systems

KYNDRA L. BUGLIONE*

National Weather Center Research Experiences for Undergraduates Program
Norman, Oklahoma
Montana State University
Bozeman, Montana

DAVID J. BODINE

OU/ARRC
Norman, Oklahoma

RACHAEL N. CROSS

OU/SoM
Norman, Oklahoma

MORGAN E. SCHNEIDER

OU/SoM
Norman, Oklahoma

ABSTRACT

Although the warning performance for supercell tornadoes has greatly improved, it is generally less adequate for quasi-linear convective systems (QLCSs). Recent studies have demonstrated that differential reflectivity (Z_{DR}) columns can be used as a proxy for updraft intensity and may help anticipate tornado formation within supercells. This study analyzes Z_{DR} column in 54 QLCS mesovortices to further investigate their potential to indicate tornado formation and intensity within QLCSs. A series of Z_{DR} column cases associated with both tornadic and nontornadic mesovorticies were studied by quantifying the height and width of each column at multiple instances prior to tornadogenesis. When comparing the width of the Z_{DR} columns between tornadic and nontornadic cases, the tornadic Z_{DR} column were slightly wider on average than the nontornadic Z_{DR} columns. More studies with a larger sample size and more statistical analysis are needed to verify this correlation. However, the initial results indicate that the width of the Z_{DR} column could potentially be useful to forecasters when predicting tornadoes in QLCSs, especially when paired with other polarimetric radar signatures. Comparing the height of the Z_{DR} columns for tornadic and nontornadic cases, there was not a distinguishable difference between tornadic and nontornadic cases or different intensities. Although most of the correlations were not incredibly consistent across all the Z_{DR} column cases, the initial results show somewhat promising correlations when looking at the Z_{DR} column width as an precursor to tornado formation and should be studied further in future research.

1. Introduction

Nearly 25% of all tornadoes occur in quasi-linear convective systems (QLCSs), yet they still impose a challenge to forecasters despite the recent improvements in tornado prediction techniques (Trapp et al. 2005). With a large emphasis placed on improving the warning performance for tornadoes in supercells, tornadoes in less discrete structures, like QLCSs, are less understood. QLCSs are convective systems built from short-lived, highly interacting cells (Trapp et al. 2005). Generally characterized by their continuous, linear structure (Fig. 1), QLCSs exhibit behaviors that are much different than discrete supercells. Tornado occurrences within QLCSs are usually weaker and shorter lived compared to supercellular tornadoes (Trapp et al. 2005). However, their tendency to occur at night induces difficulty for spotters locating possible tornado occurrences (Trapp et al. 2005). As a result, operational forecasters have difficulty providing longer lead

---

Corresponding author address: Kyndra Buglione, Montana State University, 120 David L. Boren Blvd., Norman, OK 73072, USA
E-mail: kyndra.buglione@gmail.com
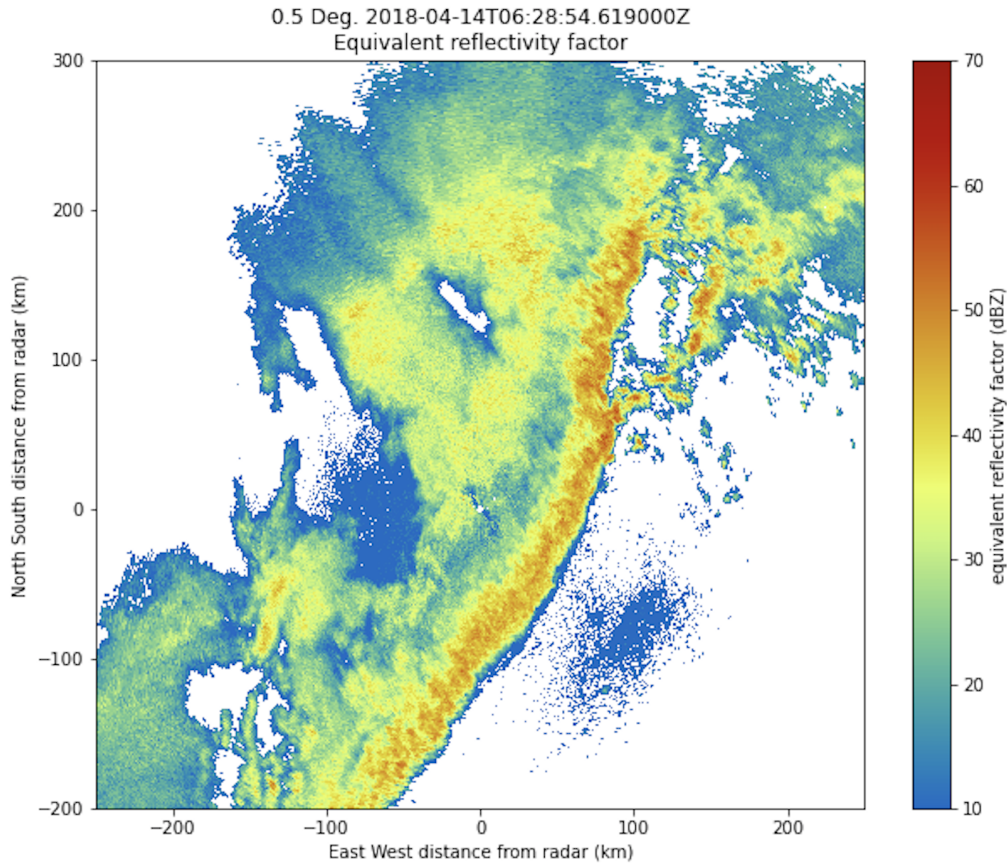
FIG. 1. Radar reflectivity factor (Z_H) of a quasi-linear convective system (QLCS) occurring on April 13th, 2018, across the state of Louisiana.

times on tornado warnings. On average, the lead times for tornadoes in QLCSs are about 4.8 minutes shorter than supercells (Brotzge et al. 2013). As an outcome of this, surrounding populations are less likely to be prepared in the event of these tornadoes and are more vulnerable during QLCSs nighttime occurrences. To improve lead times for tornado warnings in QLCSs, we can adapt processes used to identify tornadoes in supercells and analyze how they anticipate tornadoes in QLCSs.

Updraft characteristics are vital indications that a supercellular tornado is forming. Recent studies (Trapp et al. 2017; Sessa and R. J. Trapp 2020; Marion and R. J. Trapp 2021) show that the size of an updraft is a good estimate of tornado intensity for most cases. Since wider tornadoes tend to cause more damage with their larger paths, anticipating the size of a tornado can estimate its intensity. Stronger, wider tornadoes generally form with larger areas of circulation, which associated with wider mesocyclones (Trapp et al. 2017). This is because the area of circulation within the mesocyclone is limited by the width, or radius, of the updraft (Trapp et al. 2017). In turn, the

mesocyclone size reflects the scale of the updraft (Trapp et al. 2017); therefore, features of an updraft can be useful in predicting the intensity of a mesocyclone.

Although updraft characteristics are often studied within supercells, they are not as widely understood in QLCSs, making it more difficult for forecasters to predict the occurrence of QLCS tornadoes. QLCSs often have multiple mesovortices that form throughout the convective system, and they tend to be more transient than supercell mesocyclones (Marion and R. J. Trapp 2021; Sessa and R. J. Trapp 2020). With the tendency of QLCS vortices to be less persistent, the strength and lifetime of QLCS updrafts are shorter compared to supercells (Marion and R. J. Trapp 2021). Correlating with these patterns in low-level updraft strength, tornadoes in QLCSs generally have lower damage ratings on the Enhanced Fujita (EF) scale and do not last as long as supercell tornadoes (Trapp et al. 2005). Although rotating updrafts in QLCSs are generally weaker than supercells, the formation of QLCS mesovortices may still be similar to supercells when looking at the parent storm (Sessa and R. J. Trapp 2020). Using radars

to analyze similar updraft characteristics to supercells can help gain a better understanding of updrafts and tornadoes within QLCSs.

Recent improvements in radar technologies have been investigated to help enhance the forecast of tornado formations by estimating the characteristics of updrafts within supercells. Radars operate by transmitting electromagnetic (EM) radiation and receiving the reflections as they return from encountering various types of particles, such as rain and hail. For conventional radars, the EM wave is polarized in the horizontal direction to read the reflected energy in the horizontal plane (Kumjian 2013a). The use of radar measurements has greatly advanced our understanding of convective systems. Variables such as reflectivity and velocity can indicate a storm's behavior by providing information about the precipitation characteristics and motion (Kumjian 2013a). In recent years, the upgrade to dual-polarimetric radars has expanded on these processes with the ability to measure the differences in the horizontal and vertical characteristics of a target (Kumjian 2013a). Simultaneously receiving information on both planes, dual-polarimetric radars reveal the sizes of raindrops, intensity of precipitation, and types of hydrometeors. By identifying spatial and temporal changes in different radar variables, the formation of a tornado can be better anticipated.

Observing a combination of polarimetric radar signatures, forecasters can estimate the updraft intensity to anticipate a future tornado. Multiple radar signatures have been used to locate the updraft of supercells, such as differential reflectivity (Z_{DR}) columns and Z_{DR} arcs (Kumjian and Ryzhkov 2008; Kumjian 2013b). Z_{DR} is the logarithmic ratio of the reflectivity factors from the horizontally and vertically polarized echoes received (Kumjian 2013a). Obtaining measurements from both planes provides valuable information on the characteristics of hydrometeors in convective systems. It is especially useful in locating hydrometeor size sorting processes within convective systems (Kumjian 2013b). To locate the updrafts within QLCSs, this study will primarily focus on Z_{DR} columns and their relation to tornado updrafts and indicate tornado formation.

Z_{DR} columns are characterized by a narrow, vertical extension of high Z_{DR} within a mesocyclone and develop as large drops are lifted by the updraft above the environmental freezing level without freezing instantaneously (Kumjian and Ryzhkov 2008; Kumjian 2013b). As they are extended upwards, high Z_{DR} values appear in small, localized areas above the freezing level, usually surrounded by lower Z_{DR} values that indicate the presence of ice (e.g. graupel, hail, snow; Fig. 2). Therefore, Z_{DR} columns have been used as a proxy for updraft characteristics of a mesocyclone, helping to predict intensity of a tornado just before the formation has occurred (Snyder et al. 2015; French and Kingfield 2021). Additionally, Z_{DR} columns
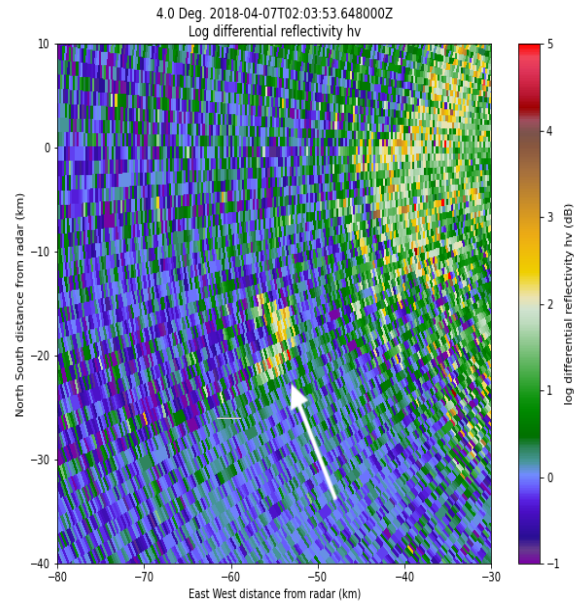
FIG. 2. Differential reflectivity (Z_{DR}) column associated with a mesovortex during a quasi-linear convective system (QLCS) that occurred on April 6th, 2018, across the state of Louisiana.

can model the behaviors of updrafts to further anticipate when the convective system is intensifying and decaying (Kumjian and Ryzhkov 2008). After predicting the general behavior of the updraft, the tornado intensity can be anticipated as the width of the vortex is related to the updraft's horizontal area (Trapp et al. 2017). By analyzing the heights and widths of multiple Z_{DR} column cases, we will observe Z_{DR} column relationships to predict tornado formation and intensity within QLCSs.

2. Data and Methods

Data Collection

The dates and times of QLCS cases were selected from the Verification of the Origins of Rotation in Tornadoes Experiment Southeast (VORTEX-SE) 2018 field campaign. Since QLCSs commonly appear in the southeastern United States (Trapp et al. 2005), three of the selected cases occurred throughout Alabama and Louisiana, while the fourth case extended farther into the midwestern region, such as Missouri. The VORTEX-SE QLCS cases were selected with the definition of a QLCS being a region of reflectivity greater than 35 dBZ that spanned over the length of 100 km (Trapp et al. 2005). After selecting the QLCS cases, Next Generation Weather Radar (NEXRAD) archive data was obtained using the NOAA Weather and Climate Toolkit (WCT) to analyze the radar characteristics of each convective system, such as reflectivity (Z_H), Doppler velocity (V_t), correlation coefficient (CC), and

Date	NEXRAD Radar Location	Damage Rating	Time (UTC)
20 Mar 2018	KHTX	EF0	0003-0032
20 Mar 2018	KBMX	EF3	0031-0102
20 Mar 2018	KBMX	EF1	0050-0123
20 Mar 2018	KFFC	EF2	0201-0225
20 Mar 2018	KFFC	EF0	0250-0311
3 Apr 2018	KILN	EF0	2040-2114
3 Apr 2018	KILN	EF1	2131-2203
3 Apr 2018	KPAH	EF2	2147-2217
3 Apr 2018	KPAH	EF0	2218-2247
3 Apr 2018	KPAH	EF1	2224-2258
3 Apr 2018	KPAH	EF2	2245-2314
7 Apr 2018	KSHV		0006-0031
7 Apr 2018	KDGX	EF1	0040-0112
7 Apr 2018	KSHV	EF1	0140-0214
7 Apr 2018	KDGX	EF1	0153-0227
7 Apr 2018	KDGX		0219-0246
7 Apr 2018	KDGX		0334-0401
7 Apr 2018	KPOE	EF1	0542-0617
14 Apr 2018	KSGF	EF0	0042-0013
14 Apr 2018	KLZK	EF1	0139-0213
14 Apr 2018	KSHV	EF1	0337-0404
14 Apr 2018	KSHV	EF2	0528-0558
14 Apr 2018	KSHV	EF1	0615-0647
14 Apr 2018	KSHV	EF1	0622-0703
14 Apr 2018	KSHV		0642-0714

TABLE 1. Table of all tornadic cases used in this study. Listed are the dates and times of each tornado report, the radar location used, and the damage rating.

differential reflectivity (Z_{DR}). The NEXRAD files were imported into a Python program using the Python ARM Toolkit (Py-ART) to view the radar data (Helmus J.J. Collis 2016). When locating Z_{DR} columns corresponding with tornado occurrences, tornado reports were used from the Storm Prediction Center (SPC) archive weather event summaries data. Soundings from the University of Wyoming atmospheric sounding archives were also viewed to obtain values of the freezing levels for each convective system (University of Wyoming College of Engineering cited 2022).

Z_{DR} Column Cases

The Z_{DR} columns were identified in two ways within each QLCS case: first, at the location of tornado reports, and second, at areas of strong rotation not associated with a tornado report. The Z_{DR} column cases that were associated with a tornado were located by using the latitude and longitude coordinates of each tornado report from the SPC. After locating the position of the tornado report on the PPI scans, a series of Z_{DR} scans were analyzed to find a Z_{DR} column in proximity of each tornado report (Fig.

3a,b). This study analyzed a total of 25 tornadic Z_{DR} column cases, which consisted of multiple EF0 and EF1 rated tornadoes on the Enhanced Fujita (EF) scale (Table 1).

Similarly, nontornadic Z_{DR} column cases were identified by locating areas containing a strong rotation of a mesovortex that were not associated with a tornado report (Fig. 3c,d). Nontornadic cases were analyzed from the same QLCSs that produced tornadoes to attempt to differentiate tornadic and nontornadic circulations. The time in which the vortices had a maximum rotational velocity was established as the time of occurrence for each nontornadic case. A total of 29 nontornadic cases were analyzed by looking at multiple scan heights and times for each area of strong rotation to locate Z_{DR} column that were in proximity of the vortices.

Z_{DR} Column Identification

The parameters established for the Z_{DR} column cases used in this study were derived using the definition of a Z_{DR} column being a narrow column of high Z_{DR} values that extends above the environmental 0°C level (Kumjian et al. 2014; Snyder et al. 2015). Specifically, the Z_{DR} columns cases established contained a small region of Z_{DR} > 1.0 dB that was surrounded by relatively low Z_{DR} values, while also appearing above the environmental freezing (0°C) level of each storm (Fig 2a,c). If the pocket of high Z_{DR} values extended across multiple scans for a considerable amount of time (i.e., 30 minutes), it was classified as a Z_{DR} column case. Other polarimetric signatures, such as high reflectivity factor values (i.e., Z_H > 45 dBZ), were also used to verify the presence of each Z_{DR} column.

In addition, cases were also determined by the quality of data available at the specific locations. For example, some tornado reports were located too far from any surrounding radar sites, so the differential reflectivity data became too coarse to identify Z_{DR} columns. Contrarily, other Z_{DR} columns were located too close to the radar and the measurements of height and width became inaccurate. This was because the highest scan did not reach above the 0°C level or the top of the Z_{DR} column, causing the height and width measurements of each Z_{DR} column to be skewed. To control the data quality, Z_{DR} column cases were chosen at distances approximately greater than 20 km but less than 150 km from the nearest radar.

Z_{DR} Column Calculations

To estimate the intensity of the updrafts associated with the Z_{DR} columns, the width and height of the individual Z_{DR} columns were recorded across their respective lifespans. The maximum height was found by looking through each radar scan elevation at the time of a Z_{DR} column occurrence to find which scan tilt was the last to contain the pocket of Z_{DR} values greater than 1 dB. Using the distance from the radar as well as the elevation angle of the radar,
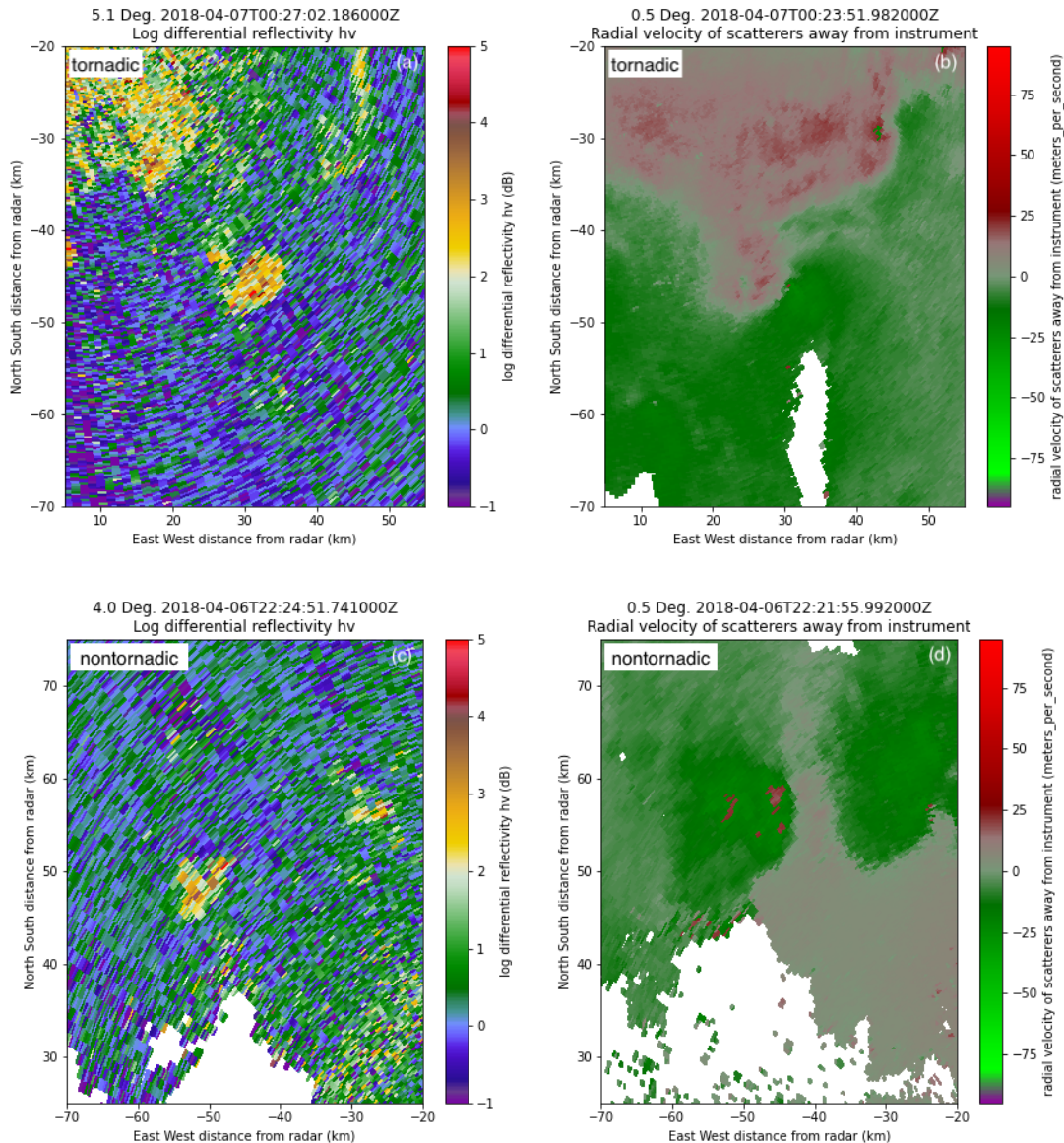
FIG. 3. Examples of a tornadic and a nontornadic Z_{DR} column. Shown are (a) a differential reflectivity (Z_{DR}) scan containing the tornadic Z_{DR} column case associated with an EF2 tornado report, (b) a radial velocity scan of the tornadic case, (c) a Z_{DR} scan containing a nontornadic Z_{DR} column case associated with a nontornadic mesovortex, and (d) a radial velocity scan of the nontornadic case.

a general estimation for the maximum height above the ground was calculated based off radar ranges for each angle. Subtracting the height of the 0°C level from the height of the Z_{DR} column above the ground, the maximum height that the Z_{DR} column extended above the 0°C level was calculated. The width of each Z_{DR} column was determined by locating the scan elevation that contained the widest portion of the Z_{DR} column and calculating the width from the PPI. Each of these steps were performed at 10 minutes, 20 minutes, and 30 minutes before the time of tornadogenesis

or maximum intensity of the mesovortices for each case to gain a better understanding of how the Z_{DR} columns evolve prior to the formation of QLCS tornadoes.

3. Results

Tornado Formation

This section compares the Z_{DR} column characteristics between tornadic and nontornadic QLCS cases. The cases
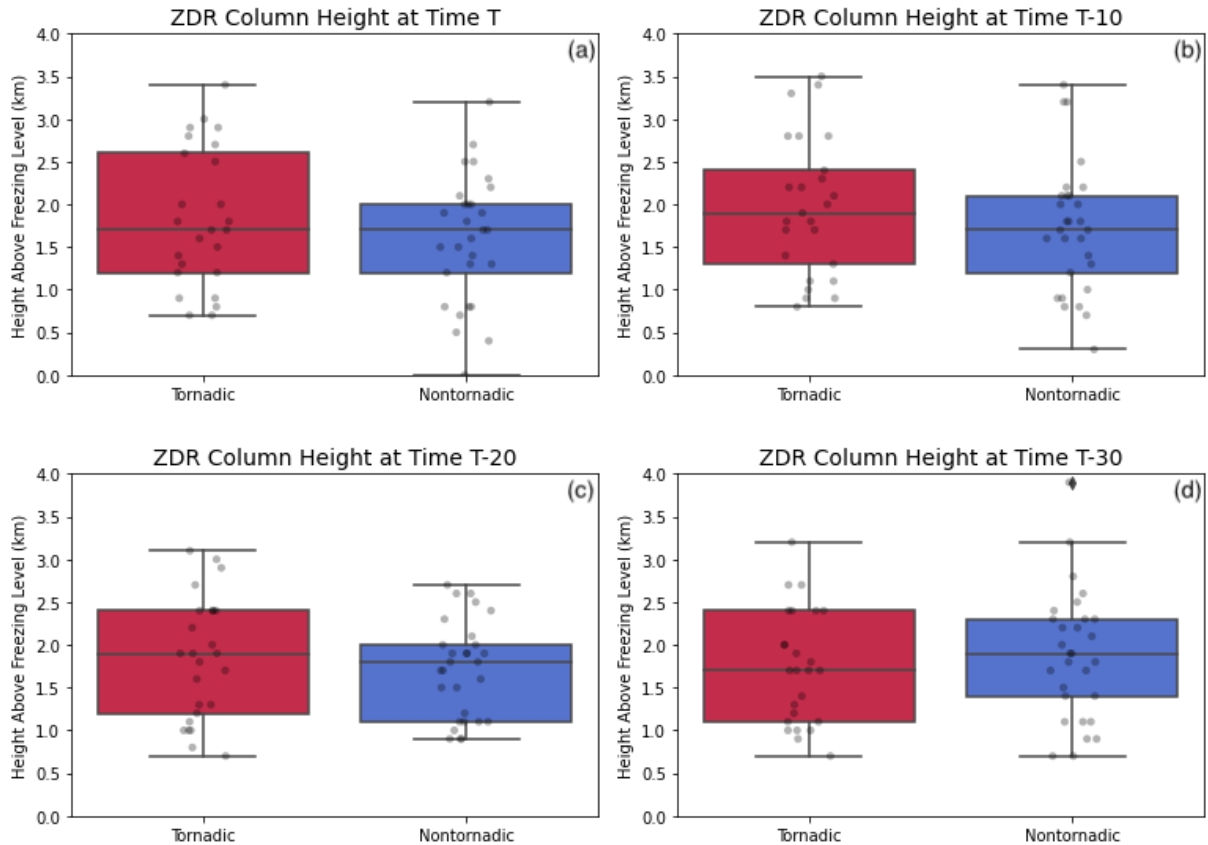
FIG. 4. Box-and-whisker plots comparing distributions of tornadic and nontornadic Z_{DR} column heights, shown (a) at time of tornadogenesis or maximum rotational velocity, (b) 10 minutes prior, (c) 20 minutes prior, and (d) 30 minutes prior to tornadogenesis.

were analyzed at the time of tornadogenesis (T), and approximately 10 minutes, 20 minutes, and 30 minutes prior (i.e., T-10, T-20, and T-30, respectively).

Comparing the maximum height of the Z_{DR} column above freezing level for the tornadic and nontornadic cases, the data indicates that there is no real distinction between the height of a tornadic or nontornadic Z_{DR} column. There is a bit of overlap between the tornadic and nontornadic cases, since the heights have a wide range of values, extending anywhere from 1 km to 3 km above the freezing level for both sets of cases (Fig. 4). The median for each time is roughly 1.7 to 1.9 km above the freezing level for both tornadic and nontornadic cases (Fig. 4). The average height for tornadic and nontornadic cases also stays relatively similar throughout each scan time, meaning there is not a noticeable trend in Z_{DR} column height leading up to tornadogenesis or maximum rotational intensity (Fig. 4).

There are a few outliers in the nontornadic cases at time T-30, with heights reaching approximately 4 km above the freezing level (Fig. 4). Although these outliers correlate with high rotational velocities, there are still other instances of high rotational velocity that did not produce

high Z_{DR} columns. There is not a clear distinction as to why the values are high compared the other nontornadic and tornadic cases, so it is just an outlier compared to the other cases of similar intensities.

Analyzing the distribution of Z_{DR} column widths of the tornadic and nontornadic cases, there is a slight difference between the tornadic and nontornadic Z_{DR} column width. Tornadic Z_{DR} columns averaged around 6.5 km in width and nontornadic Z_{DR} columns averaged around 5.5 km in width (Fig. 5). In general, the distribution of the cases does not exhibit as extensive overlap and there is a slight difference between the medians of the two cases (Fig. 5). Therefore, tornadic cases consist of a wider diameter on average in their associated Z_{DR} columns than nontornadic cases. Especially looking at the scan time of T-30, the earliest time examined, tornadic Z_{DR} columns are 1.25 km wider on average than nontornadic Z_{DR} columns (Fig. 5). Although the greatest difference in Z_{DR} column width occurred at T-30, when looking at all of the cases there is no trend in Z_{DR} width over time leading up to tornadogenesis or maximum rotational intensity. However, the differences
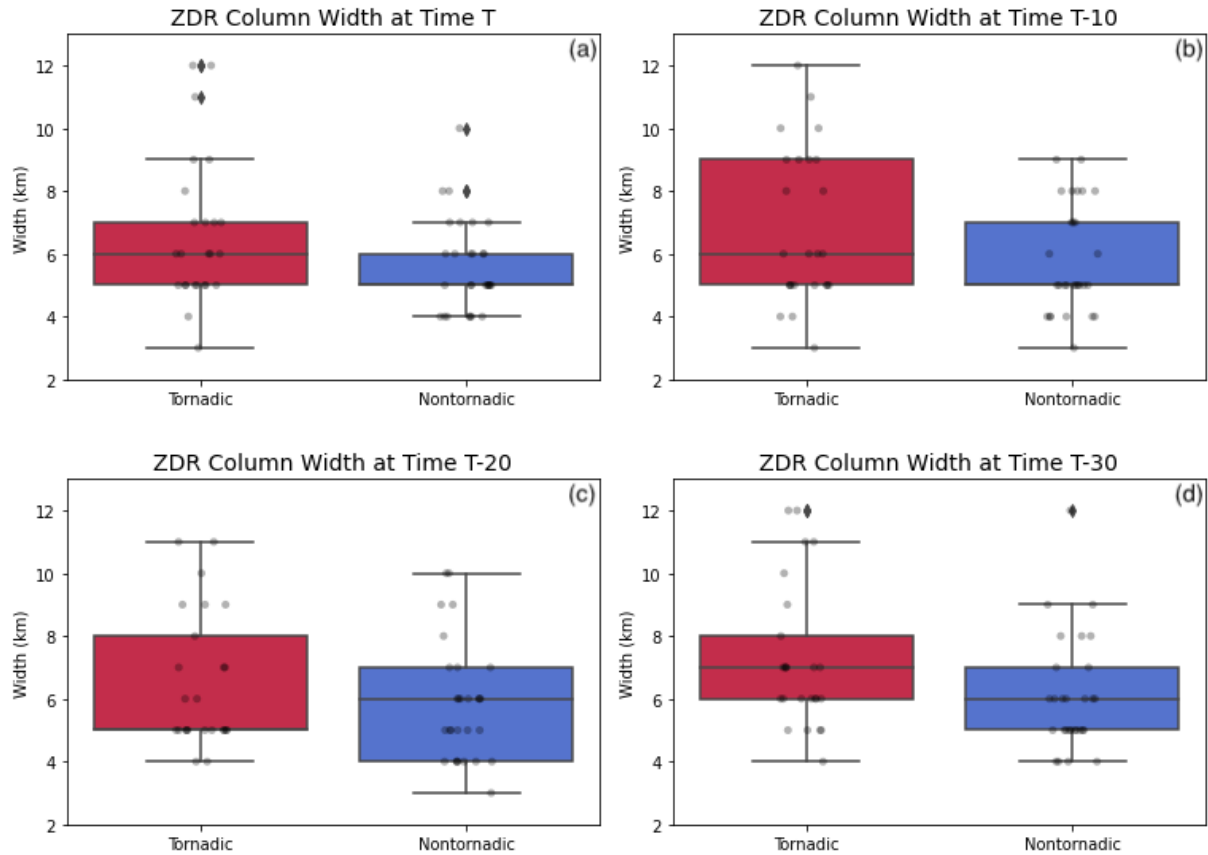
FIG. 5. Box-and-whisker plots comparing distributions of tornadic and nontornadic Z_{DR} column widths, shown (a) at time of tornadogenesis or maximum rotational velocity, (b) 10 minutes prior, (c) 20 minutes prior, and (d) 30 minutes prior to tornadogenesis.

in Z_{DR} width for tornadic and nontornadic cases should still be noted across all time scans.

Similar to the height analysis, there are a few outliers present within the data. Here, the outliers extend across both tornadic and nontornadic cases on almost all scan times (Fig. 5). When looking at the data, no correlation is found between width and maximum velocity values for the outliers.

Tornado Intensity

This section analyzes the differences in Z_{DR} column characteristics in comparison to the intensity of the tornadic and nontornadic cases. The heights and widths were analyzed at T-10 to obtain a measurement the Z_{DR} columns before tornadogenesis.

Looking at the distributions of Z_{DR} column width and height in comparison to EF scale rating of the tornadic cases, the height does increase with a greater EF rating (Fig. 6a). On average, the height of Z_{DR} columns associated with EF2+ cases are roughly 3 km high, while EF0 and EF1 tornadic cases have heights extending less than

2 km above the freezing level. However, one caveat to this analysis is the lack of EF2+ tornado reports present in QLCSs. This means the EF2+ cases compared to EF1, EF0 and nontornadic cases may not accurately represent the differences in the Z_{DR} column characteristics as a predictor of tornado intensity. To further understand if Z_{DR} column height relates to tornado intensity, more cases for EF2+ tornado occurrences in QLCSs would need to be examined.

Contrarily, the distributions of the Z_{DR} columns widths do not have any correlation with the EF rating given (Fig. 6b). The large differences in distributions for the widths of tornadic cases across the EF scale indicate that there is not a correlation with Z_{DR} column width and tornado intensity. As previously stated, the sample size of this study is not large enough to validate the correlations seen across these Z_{DR} column cases. In order to verify that there is no correlations between the intensity and the Z_{DR} column width, a larger sample size would need to be accumulated.

To attempt to increase the sample size with tornado intensity, this study also uses the maximum rotational velocity as a measurement of intensity across both tornadic
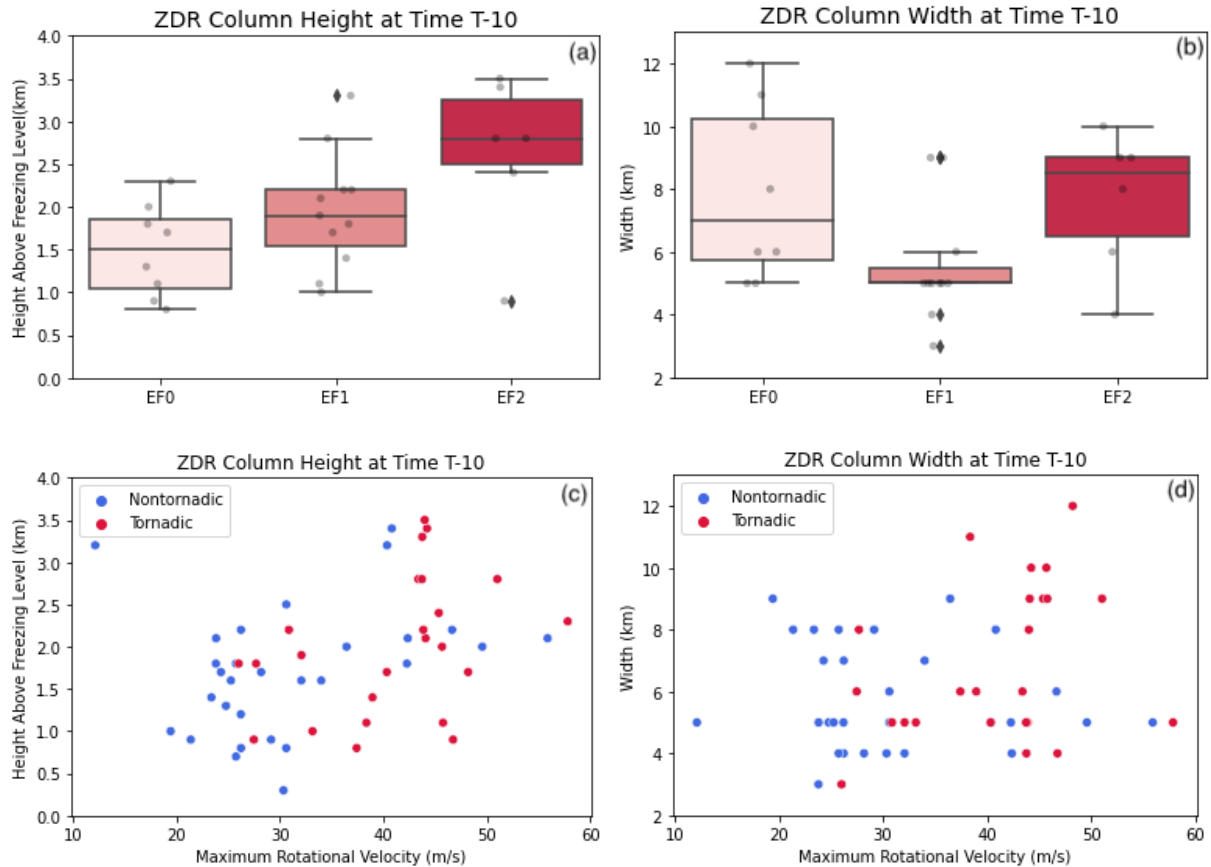
FIG. 6. Plots comparing the intensity of the mesovortices with both the heights and widths of the Z_{DR} columns. Shown are (a) box-and-whisker plot distributions of the Z_{DR} column height for each EF scale rating, (b) box-and-whisker plot distributions of the Z_{DR} column width for each EF scale rating, (c) scatter plot of the Z_{DR} column heights and the maximum rotational velocity, and (d) scatter plot of the Z_{DR} column widths and the maximum rotational velocity.

and nontornadic cases. Plotting the maximum rotational velocity along with the Z_{DR} column height and width at time T-10, it is seen that there is not a noticeable correlation with rotational velocity and Z_{DR} column width (Fig. 6b). However, looking at the Z_{DR} column heights in comparison to the rotational velocity, there could be a possible correlation between the two measurements (Fig. 6a). With further statistical analysis and a larger sample size, this could be better examined to verify the presence of this correlation.

4. Discussion

Although the height of the Z_{DR} column did not exhibit much difference between tornadic and nontornadic cases, the width of the tornadic Z_{DR} columns were slightly larger in comparison to nontornadic Z_{DR} columns. With a majority of QLCS tornadoes being much weaker and appearing for a shorter duration, it is not surprising that the differences between the tornadic and nontornadic cases are less

distinct than supercellular tornado cases. The findings of this study support those in French and Kingfield (2021) , as they studied Z_{DR} column area within supercells. They found that Z_{DR} columns can be used to predict tornado formation when applied with all other relevant forecasting information. Although most of the research presented in French and Kingfield (2021) examined the Z_{DR} column cases of higher rated tornadoes within supercells, the study also observed the differences in nontornadic cases and tornadoes with a low EF rating. When they investigated the weaker tornadic and nontornadic cases, the difference in the area of tornadic cases and nontornadic cases was very little, but still somewhat distinguishable. The results presented in French and Kingfield (2021) paralleled the results found here, as the tornadic Z_{DR} columns were on average slightly wider than nontornadic Z_{DR} columns. Since tornadoes in QLCSs are generally weaker and more transient, the prediction of tornadogenesis using Z_{DR} columns may be more challenging compared to supercells due to the reduced differences in updraft intensity.

French and Kingfield (2021) also examined the potential for Z_{DR} columns to predict the intensity of a tornado. They used the EF scale ratings issued by the SPC as well as the maximum ΔV values to measure the intensity of a tornado. Their findings resulted in a wide difference between tornadoes with an EF rating above an EF2, but like this study, the differences in the Z_{DR} column areas for the tornadoes with a lower damage rating were practically undetectable. Similarly, when looking at the rotational velocity as an indicator of intensity, the correlation between rotational velocity and Z_{DR} column area was not that strong. The results found here also supported the findings that rotational velocity and Z_{DR} column characteristics do not exhibit a major correlation with one another. Especially with weaker tornadoes that do not exhibit much difference in rotational velocities, using Z_{DR} columns to predict tornado intensity with rotational velocity in QLCSs could be more difficult for forecasters to use. Since QLCS tornadoes are typically weaker than supercellular tornadoes, the characteristics of Z_{DR} columns alone are not necessarily a viable indication of tornado intensity within QLCSs.

An added complication of this study was the quality of radar data presented. The NEXRAD system provides high quality data, especially in the southeastern regions. However, there are always areas that the radar does not scan high enough or is obstructed from view, preventing a good quality scan of certain regions. Especially since QLCSs span over the length of multiple radar locations, there are considerable areas within each convective system where quality radar data is not obtainable. Another limitation with using NEXRAD data is that the radars only scan every 5-7 minutes. Therefore, if a Z_{DR} column changes drastically over the course of 5 minutes, the radar would not detect the difference fast enough, if at all, to notify forecasters. These radar limitations have a huge effect on the ability to use Z_{DR} columns to predict tornado formation and intensity within QLCSs. To possibly improve these limitations, Z_{DR} columns should also be examined in mobile radar data to obtain faster scans and higher quality radar data. Although the initial results found here might be a challenge for forecasters, Z_{DR} columns should still be investigated further to become a useful indication when predicting tornadoes in QLCSs.

5. Conclusion

Lead times for tornado warnings in QLCSs have improved little compared to supercells. Since QLCSs tend to produce tornadoes at night, more challenges are forecasters when alerting the public of QLCS tornado occurrences. To help increase the warning performance of QLCS tornadoes, similar processes used to predict tornadoes in supercells can be examined within QLCSs. This study focused on using Z_{DR} columns as a proxy for updraft characteristics to better predict the formation and intensity of tornadoes within QLCSs. We analyzed the height and width of each Z_{DR} columns at multiple instances leading up to tornadogenesis to find correlations between different characteristics of Z_{DR} columns and QLCS tornadoes.

The difference in Z_{DR} column heights was not distinguishable between tornadic and nontornadic cases at any time before tornadogenesis or maximum intensity. This means that the height of a Z_{DR} column is not a good indicator of a tornadic or nontornadic mesovortex. However, the Z_{DR} column widths associated with tornadic mesovorticies were slightly larger than those not associated with tornadic mesovorticies. Although the tornadic Z_{DR} column cases were only around 1 km larger than nontornadic cases, the difference could still be enough to verify the presence of a tornadic mesovortex. With further research using a larger sample size and more statistical analysis, the Z_{DR} column width could potentially help forecasters predict the formation of QLCS, especially when paired with other polarimetric radar signatures.

References

Brotzge, J. A., S. E. Nelson, R. L. Thompson, and B. T. Smith, 2013: Tornado probability of detection and lead time as a function of convective mode and environmental parameters. *Wea. Forecasting*, **28**, 1261–1276, doi:10.1175/waf-d-12-00119.1.

French, M. M., and D. M. Kingfield, 2021: Tornado formation and intensity prediction using polarimetric radar estimates of updraft area. *Wea. Forcasting*, **36**, 2211–2231, doi:10.1175/waf-d-21-0087.1.

Helmus J.J. Collis, S., 2016: The python arm radar toolkit (py-art), a library for working with weather radar data in the python programming language. *Journal of Open Research Software*, p.e25, doi: https://doi.org/10.5334/jors.119.

Kumjian, M. R., 2013a: Principles and applications of dual-polarization weather radar. part i: Description of the polarimetric radar variables. *J. Operational Meteor*, **1(19)**, 226242, doi:http://dx.doi.org/10.15191/nwajom.2013.0119.

Kumjian, M. R., 2013b: Principles and applications of dual-polarization weather radar. part ii: Warm- and cold-season applications. *J. Operational Meteor*, **1(20)**, 243264, doi:http://dx.doi.org/10.15191/nwajom.2013.0120.

Kumjian, M. R., A. P. Khain, N. Benmoshe, E. Ilotoviz, A. V. Ryzhkov, and V. T. Phillips, 2014: The anatomy and physics of zdr columns: Investigating a polarimetric radar signature with a spectral bin microphysical model. *J. Appl. Meteor. Climatol.*, **53**, doi:10.1175/jamc-d-13-0354.1.

Kumjian, M. R., and A. V. Ryzhkov, 2008: : Polarimetric signatures in supercell thunderstorms. *J. Appl. Meteor. Climatol*, **40**, 1940–1961, doi:10.1175/2007jamc1874.1.

Marion, G. R., and . R. J. Trapp, 2021: Controls of quasi-linear convective system tornado intensity. *J. Atmos. Sci.*, **78**, 1189–1205, doi: 10.1175/jas-d-20-0164.1.

Sessa, M. F., and . R. J. Trapp, 2020: Observed relationship between tornado intensity and pretornadic mesocyclone characteristics. *Wea. Forecasting*, **35**, 1243–1261, doi:10.1175/waf-d-19-0099.1.

Snyder, J. C., A. V. Ryzhkov, M. R. Kumjian, A. P. Khain, and J. Picca, 2015: A zdr column detection algorithm to examine convective storm updrafts. *Wea. Forecasting*, **30**, 1819–1844, doi: 10.1175/waf-d-15-0068.1.

Trapp, R. J., G. R. Marion, and S. W. Nesbitt, 2017: The regulation of tornado intensity by updraft width. *J. Atmos. Sci*, **74**, 4199–4211, doi:10.1175/jas-d-16-0331.1.

Trapp, R. J., S. A. Tessendorf, E. S. Godfrey, and H. E. Brooks, 2005: Tornadoes from squall lines and bow echoes. part i: Climatological distribution. *Wea. Forecasting*, **20**, 23–24, doi:10.1175/waf-d-15-0068.1.

University of Wyoming College of Engineering, cited 2022: Atmospheric Soundings. [Available online at https://weather.uwyo.edu/upperair/sounding.html].